Internal Bracing Requirements of Horizontally Curved Box-girders

Chai H. Yoo[1] , Junsuk Kang [2]**,** Kyungsik Kim[3]

Abstract:

The trapezoidal box (tub) girder is frequently used for horizontally curved highway bridges because of its high torsional rigidity. The developed theory of combined bending and torsion of horizontally curved thin-walled girders is based on the assumption that the girder cross-section retains its original shape. To achieve this, the girder must be braced by means of sufficiently closely spaced diaphragms, which are supposed to be infinitely stiff. The bracing frequently employed in the form of transverse lattice systems does fulfill this requirement to some degree. Analytical studies, however, have shown that a box-girder subjected to torsional loading undergoes cross-sectional deformation. This gives rise to longitudinal stresses due to distortional warping and transverse bending stresses due directly to deformation of the cross section. These stresses tend to reduce the advantage anticipated from the high torsional rigidity of the box-girder. A means and method of evaluating these stresses have been developed. It has been demonstrated that the developed procedure is satisfactory in meeting the specification requirements to check these stresses.

1.   Introduction

Intermediate internal cross-frames were once a very obscure topic. In fact, the latest edition of AASHTO Standard Specifications for Highway Bridges (AASHTO, 2002) stipulates that "intermediate cross-frames are not required for steel box girders designed in accordance with this specification." They are, however, permitted to be installed on a temporary basis for handling and erection purposes. The Guide Specifications for Horizontally Curved Highway Bridges (AASHTO, 1980) gave a formula to compute the cross-frame spacing with a maximum limited to 7.5 m (25 feet). It appears that the formula is based on a regression analysis with limited parameters. Article 6.7.4.3 (AASHTO, 2014) requires that intermediate internal diaphragms or cross-frames be provided for all single box sections, horizontally curved sections, and multiple box sections in cross-sections of bridges not satisfying certain geometric proportions. The spacing of the internal diaphragms or cross-frames is specified not to exceed 12 m (40 feet). In the Commentary of the Article, transverse bending stresses due to cross-section distortion are explicitly limited to 140 MPa (20 ksi) and the longitudinal warping stresses (torsional warping and

---

[1] Professor Emeritus, Auburn University, chyoo@auburn.edu
[2] Assistant Professor, Georgia Southern University, jkang@georgiasouthern.edu
[3] Assistant Professor, Cheongju University, kkim@cju.ac.kr

distortional warping) due to the critical factored torsional loads are not to exceed approximately ten percent of the longitudinal stresses due to major-axis bending at the strength limit state. There is, however, no guideline is given as to what type of analysis technique is to be used to meet these requirements. It appears that a modern finite-element analysis is perceived to be a cure-all for structural analysis problems. As the finite-element analysis gives only the total stress, it becomes problematic to discern whether a design meets the specification requirements that the stress due to an action is to be within the prescribed percentage of the longitudinal stresses due to the major-axis bending at the strength limit state.

A lateral bracing system of a Warren truss with posts is usually installed at the top flange level of an open-top tub girder to form a quasi-box, thereby increasing the torsional rigidity during construction. The lateral bracing system is subjected to the noncomposite dead load as shown in Fig. 1. A general method of computing forces in the lateral bracing system was not available until Fan and Helwig (1999, 2002) presented a method. AASHTO (2014) recognizes this method in the Commentary of Article 6.7.5.3. Kim and Yoo (2006a, 2006b, 2009) refined and extended this method, including the interaction of top lateral and internal cross-frame bracing systems as shown in Figs. 2 and 3, and a quantitative guidance to the effect of installing the cross-frames at one-, two-, and three-panel spacing. In light of the modern industry preference for installing a few heavy intermediate internal cross-frames, such an information should be useful. It is of interest to note that the member force diagram of the lateral bracing is similar to the vertical bending moment diagram as the member force is controlled by shortening of the member primarily due to the flexural action, although the bracing is installed to increase the torsional rigidity. Kim and Yoo (2006b) also report that the member forces developed in the single diagonal members are 25-30 percent higher in the case when internal cross-frames are placed at odd numbered panel spacing than when it is even. Such a seemingly strange behavior pattern has been observed by Abbas et al. (2006) for corrugated web I-girders under in-plane loads when the number of web panels is odd or even. Once the concrete deck is hardened, the lateral bracing system is no longer needed. However, the stresses develop in the members of the bracing system are locked in. The skewed members of the intermediate internal cross-frame (K-frame is more common as compared to X-frame) are subjected to additional stresses due to distortion of the cross section due to noncomposite dead loads, live loads, and composite dead loads. Since Kim and Yoo have thoroughly examined the stresses due to noncomposite dead loads, this paper will focus on the distortional aspect.

Wright et al. (1968) presented an analytical procedure to determine the distortion induced stresses of straight box-girders known as the BEF (Beams on Elastic Foundation) analogy. Their model employed the vertical deflection of a web as a single degree of freedom measuring the distortion of a box section. Despite their claim to be otherwise, the developed procedure is very complex and is not easy to follow. It appears that they relied heavily on the solution of a fourth order ordinary differential equation with constant coefficients, which implies that their solution cannot be directly applied to bridge girders with variable cross-section properties. In order to alleviate the situation, Heins and Hall (1981) prepared a designer's guide to steel box-girder bridges as a Bethlehem publication with a series of figures and charts. In Europe, Dabrowski (1968, 1972) published independently a book on curved thin-walled girders, theory and analysis, which includes a chapter on box-girder distortion. His model uses the distortion angle as the single degree of freedom measuring the degree of cross-section distortion.
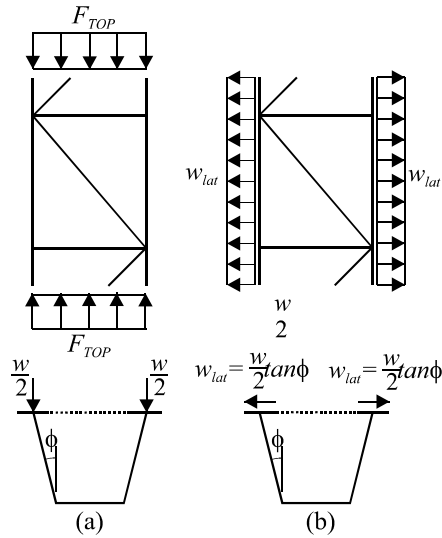
Figure 1: Forces in bracing members and top flanges (a) longitudinal components, (b) lateral components (adopted from Kim and Yoo, 2006a)
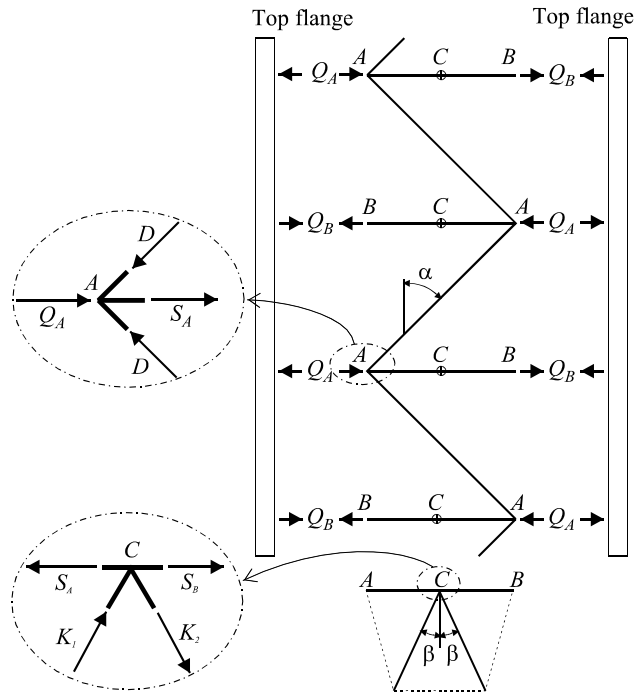
Figure 2: Interactive forces between top flanges and bracing members (adopted from Kim and Yoo, 2006b)

Despite the fact that the matrix structural analysis was well established at the time, the early two researchers of box girder distortion did not take advantage of this superb method. Rather, they relied heavily on the solution of the fourth order differential equation with constant coefficients. In order to alleviate the difficulty, they included copious charts and tables.

3
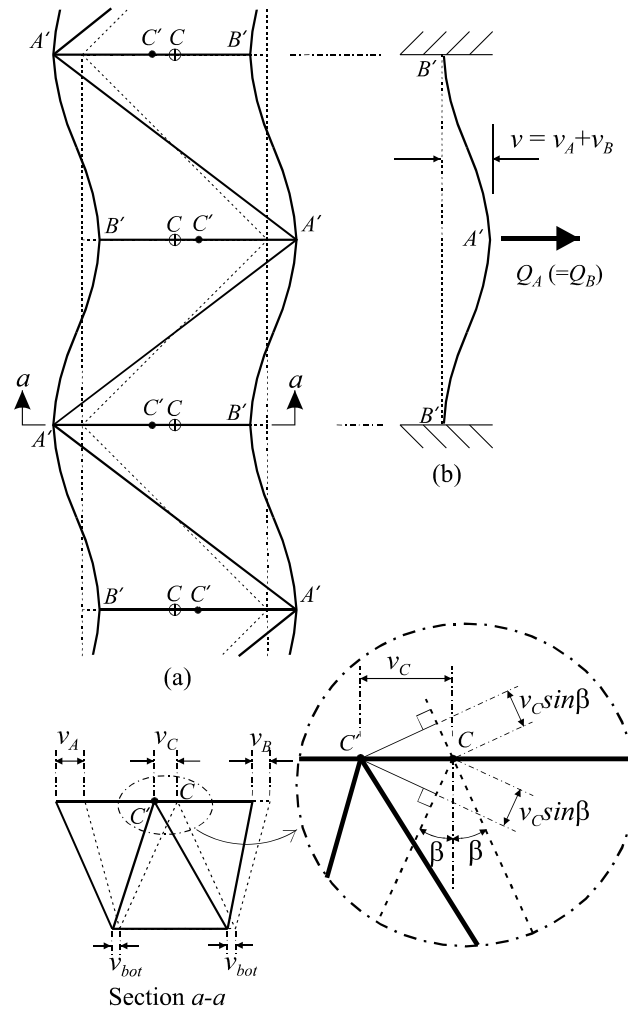
Figure 3: Assumed lateral displacements (internal K-frames) (a) Top flanges and lateral bracing members, (b) Lateral deflection of top flange (adopted from Kim and Yoo, 2006b)

The effectiveness of such charts and tables is questionable as none of the aids can be applied directly to the modern-day continuous curved box-girder bridges with variable cross-section properties. Park et al. (2003, 2005a, 2005b) and Kermani and Waldron (1993) developed beam elements with distortional degrees of freedom. Their programs cannot accommodate elastic constraints though. This can be a serious limitation. As it will be shown later, distortion can be controlled by diaphragm or cross-frame spacing and its stiffness. In fact, the stiffness of a typical cross-frame placed in a box-girder is only a very small fraction of that of a solid plate diaphragm normally placed at supports, thereby yielding considerable distortion.

Bridge design specifications (AASHTO, 2014; Hanshin, 1988) mandate the designer to keep the torsional and distortional stresses under the limiting values without any guidelines offered. The procedure that is to be detailed herein is to apply the concept of the BEF analogy directly using

4

two relatively simple computer programs. The static analysis of horizontally curved box-girders as the prerequisite to the distortion analysis is carried on a program CVSTB based on the exact curved beam element stiffness matrix Yoo (1979) developed. The moment output is used as an input in an ordinary two-dimensional plane frame analysis program. Examples (Yoo et al., 2015) demonstrate the reliability of the procedure. As all numerical calculations are carried out by the computer programs, the procedure is applicable to any combinations of loadings and boundary conditions, cross-sectional property variations, and arbitrary combinations of span lengths. Since detailed derivation of the governing equation of the BEF analogy is given in Yoo et al. (2015), this paper will present an alternate method of deriving the same governing equation by the concept of the minimum potential energy principle.

2.   Derivation of the fundamental equations for distortion

There are many properties in distortional warping defined similarly to those for torsional warping. The warping functions are

$$w_D(s) = -\int_0^s \rho(s)ds + C_1 \qquad\qquad \text{distortion} \qquad\qquad\qquad (1a)$$

$$w_T(s) = -\int_0^s \rho(s)ds + C_1 \qquad\qquad \text{torsion} \qquad\qquad\qquad (1b)$$

where ρ is the perpendicular distance measured from the distortion center and shear center to a point on the cross section, respectively; $C_1 =$ integral constant; $s =$ perimeter coordinate.

The warping constants are

$$I_{Dw} = \int_A w_D^2 dA \qquad\qquad \text{distortion} \qquad\qquad\qquad (2a)$$

$$I_{Tw} = \int_A w_T^2 dA \qquad\qquad \text{torsion} \qquad\qquad\qquad (2b)$$

where $A =$ cross-sectional area.

The warping moments are

$$M_D = EI_{Dw}\gamma'' \qquad\qquad \text{distortion} \qquad\qquad\qquad (3a)$$

$$M_T = EI_{Tw}\phi'' \qquad\qquad \text{torsion} \qquad\qquad\qquad (3b)$$

where $E =$ modulus of elasticity; $\gamma =$ distortion angle; $\phi =$ torsional rotation.

The warping normal stresses are

$$\sigma_{Dw} = \frac{M_{Dw}w_D}{I_{Dw}} \qquad\qquad \text{distortion} \qquad\qquad\qquad (4a)$$

$$\sigma_{Tw} = \frac{M_{Tw}w_T}{I_{Tw}} \qquad\qquad \text{torsion} \qquad\qquad\qquad (4b)$$

Consider a singly symmetrical trapezoidal section shown in Fig. 4 where $a =$ length of the overhang; $b = .$distance between top flanges; $c =$ width of the bottom flange; $h =$ height of the section; $D =$ distortion center; $\beta =$ parameter to determine the location of the distortion center. For a singly symmetrical cross-section, the distribution of the distortional warping function is anti-symmetrical, as shown in Fig. 4, and the distortional warping function is zero on the axis of symmetry. The distortional warping function at the top of the web of the general trapezoidal box section is given by Dabrowski (1972) and Yoo et al. (2015) as

$$w_{D1} = \frac{hb^2c}{2(b+c)(\beta b+c)} \tag{5}$$

For a rectangular box section where $b = c$, Eq. (4) yields $w_{D1} = bh/[4(1+\beta)]$, which is the same as that presented by Nakai and Murayama (1981).

It can be shown (Yoo et al., 2015) that

$$w(z,s) = \frac{d\gamma(z)}{dz} w_D(s) \tag{6}$$

It follows immediately that the distortional normal stress is given by

$$\sigma_{Dw} = E\varepsilon = E\frac{\partial w}{\partial z} = E\frac{d^2\gamma}{dz^2} w_D \tag{7}$$

Since the distortion does not produce any additional axial force N_z, or bending moments M_x and M_y, the following equations must be met:

$$N_z = \int_A \sigma_{Dw} dA = 0 \tag{8a}$$

$$M_x = \int_A \sigma_{Dw} y dA = 0 \tag{8b}$$

$$M_y = \int_A \sigma_{Dw} x dA = 0 \tag{8c}$$

Because w_D is antisymmetric with respect to the y axis, Eqs. (8a) and (8b) are automatically satisfied.

Eq. (8c) gives the location of the distortion center D for the general case of open closed cross-section shown in Fig. 4. Let A_{u1}, A_u, A_{u0}, A_v, and A_l be the areas of the steel top flange, equivalent entire upper deck, top deck excluding overhangs, web, and lower steel flange, respectively. A_u may be replaced by $A_{u0}(1+2a/b)$. Using Eq. (8c), the parameter β is determined as

$$\beta = \frac{b\left[A_u\left(1+\frac{2a}{b}\right)^2 + 6A_{u1}\right] + 2A_v b + A_v c}{A_l c + 2A_v c + A_v b} \tag{9}$$

Eq. (9) can be used for other cases of open-closed or closed sections. For closed sections, let the overhang length a be equal to zero and for rectangular box sections, let c equal to b in Eq. (9).

In the analysis of the lattice-type cross-frame shown in Fig. 5, the perimeter members are conservatively assumed not to participate in resisting the lateral displacement. The cross-sectional deformation occurs as the result of extensional deformation of the inner members. The stiffness K_1 of a cross-frame is defined as that value of the product $S_l h$ to which a deformation angle γ of unit magnitude corresponds. The value of the cross-frame stiffness can be determined by considering the energy equations. The internal energy is given by $1/2\ K_1\gamma^2$. The external energy

6

is equal to $1/2\ S_l u_l = /2\ S_l h\gamma$ while the other components of u_u, v_1, and v_2 must be zero. Hence $1/2\ K_1\gamma^2 = 1/2\ S_l h\gamma$, so that
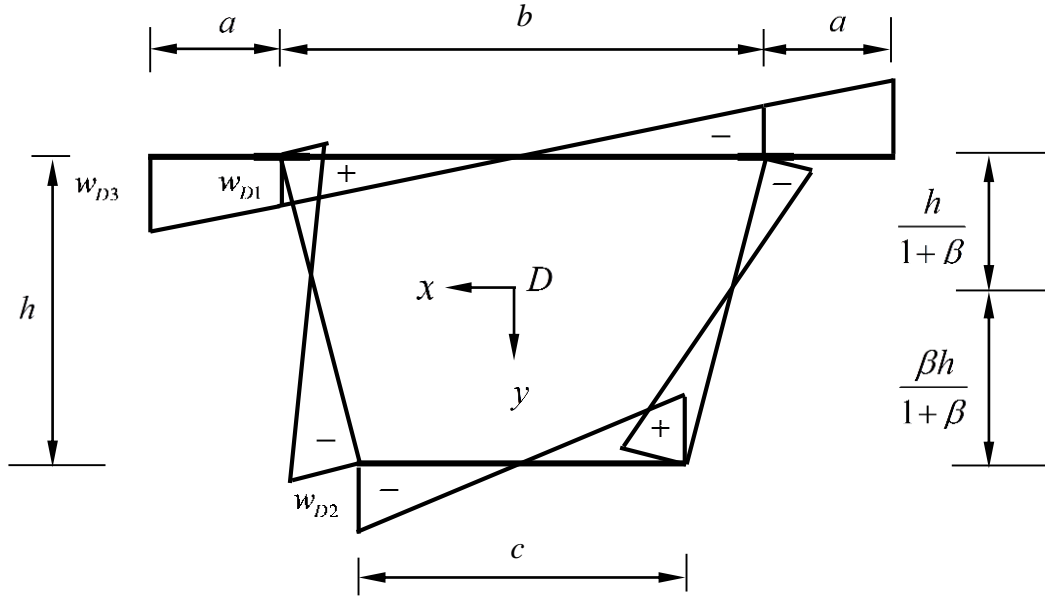
Figure 4: Distortional warping function in trapezoidal composite section (adopted from Yoo et al., 2015)
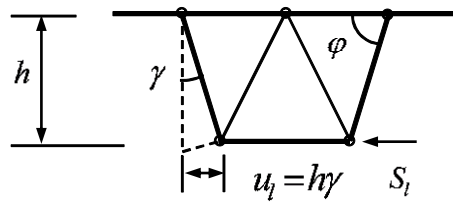
Figure 5: Deformation of cross-frame (adopted from Yoo et al., 2015)

$$\gamma = \frac{S_l h}{K_1} \qquad (10)$$

The stiffness per unit length in the z-direction is equal to

$$k_1 = \frac{K_1}{l_D}$$

where l_D is the distance between the adjacent cross-frames. The "smear out" operation may be conducive to construct the governing differential equation, it is not recommended as this operation destroys the detailed picture of the effect of placing internal cross-frames.

Here, K_1, the stiffness of the internal cross-frames against the distortion can be estimated as follows (Nakai and Yoo, 1988; Yoo et al., 2015):
For a plate type

$$K_1 = Gt_D bh \qquad \text{(rectangular box)} \quad K_1 \doteq \frac{Gt_D(b+c)h}{2} \quad \text{(trapezoidal box)} \tag{11a}$$

For a truss type
      X type

$$K_1 = \frac{2EA_b b^2 h^2}{\ell_b^3} \quad \text{(rectangular box)} \quad K_1 = \frac{EA_b(b+c)^2 h^2}{2\ell_b^3} \quad \text{(trapezoidal box)} \tag{11b}$$

      K type

$$K_1 = \frac{EA_b b^2 h^2}{2\ell_b^3} \quad \text{(rectangular box)} \quad K_1 = \frac{EA_b c^2 h^2}{2\ell_b^3} \qquad \text{(trapezoidal box)} \tag{11c}$$

For a frame type

$$K_1 = \frac{24EI_v}{\alpha_0 h} \tag{11d}$$

where G = shear modulus; t_D = thickness of diaphragm; A_0 = cross-sectional area of truss member; ℓ_b = length of truss member. In Eq. (11d), α_0 can be evaluated from Eq. (13) provided that the moment of inertia of the web I_v is determined by taking into account the effective width b_m according to the spacing of the internal diaphragm ℓ_D as follows:

$$b_m = \begin{cases} d/3 & \text{for } \ell_D \geq d/3 \\ \ell_D & \text{for } \ell_D < d/3 \end{cases} \tag{12}$$

Here d is the smaller of the width b or the height h of the box.
In a similar manner, the stiffness of the box (considered as a closed frame) of unit width is

$$k_1 = \frac{24EI_v}{\alpha_0 h} \quad \text{with} \quad \alpha_0 = 1 + \frac{2\dfrac{b}{h} + 3\dfrac{I_u + I_l}{I_v}}{\dfrac{I_u + I_l}{I_v} + 6\dfrac{h}{b}\dfrac{I_u I_l}{I_v^2}} \tag{13}$$

where I_u = moment of inertia of the top deck; I_l = moment of inertia of the bottom flange
Timoshenko (1955) shows the derivation of the expression of α by a frame analysis.
Wright et al. (1968) stated that "Because the behavior of the box cell proves to be insensitive to minor variations in diaphragm (cross-frame) stiffness, it is permissible to use the equation developed for a rectangular box for a trapezoidal box." As will be shown later in the **Major design example**, the frame stiffness, k_1 is in the order of 1/1,000 of the cross-frame stiffness, K_1. Doubling or tripling k_1 hardly affects the analysis results, thereby justifying the assumption employed by Wright et al. (1968).

Considering equilibrium of torsional moments on a curved infinitesimal, one obtains immediately

$$\frac{dM_z}{dz} - \frac{M_x}{R} = -m_z \quad \text{or} \quad -\frac{dM_z}{dz} = m_z - \frac{M_x}{R} \tag{14}$$

Because of the non-collinearity of the resultant forces due to vertical bending, radial forces act upon the webs and flanges. Reflecting these forces, Dabrowski (1972) gives the following expression for the applied torque and corresponding angular distortion:

$$\gamma = \frac{1}{k_1}\left(-\frac{\eta M_x}{R} + m_z^*\right) \tag{15}$$

with

$$\eta = \alpha_1 - \frac{\alpha_2}{\alpha_0} \tag{16}$$

where

$$\alpha_1 = \frac{7h_u - 3h_l}{10I_x}h^2 t_v + \frac{A_u h_u h}{I_x} - \frac{1}{2} \tag{17}$$

and

$$\alpha_2 = \frac{ht_v}{15I_x}\left[\frac{\left(3h_u - 2h_l\right)\left(b + 3h\frac{I_l}{I_v}\right) + \left(3h_u - 2h_l\right)\left(b + 3h\frac{I_u}{I_v}\right)}{\left(\frac{I_u + I_l}{I_v}\right) + 6\left(\frac{h}{b}\right)\left(\frac{I_u I_l}{I_v^2}\right)}\right] \tag{18}$$

It appears that Dabrowski [4] overlooked the negative sign in Eq. (15) in his original derivation.

The strain energy U_σ due to the distortional warping stress σ_{Dw} is

$$U_\sigma = \frac{1}{2E}\int_0^\ell\int_A \sigma_{Dw}^2\, dA\, dz = \frac{1}{2}\int_0^\ell\int_A\left(\frac{\partial w}{\partial z}\right)^2 dA\, dz = \frac{E}{2}\int_A w_D^2\, dA \int_0^\ell\left(\frac{d^2\gamma}{dz^2}\right)dz \tag{19}$$

where ℓ is the span length of the girder. Substituting the distortional warping constant, Eq. (2a), Eq. (19) reduces to

$$U_\sigma = \frac{EI_{Dw}}{2}\int_0^\ell\left(\frac{d^2\gamma}{dz^2}\right)^2 dz \tag{20}$$

The energy equation for the warping shear flow in the bottom flange per unit width and the corresponding distortional angle is

$$\int_0^\ell\left(\frac{1}{2}k_1\gamma^2\right)dz \tag{21}$$

Likewise, the loss of potential energy associated with the external distributed torsional moment can be summed assuming a unit displacement as

$$\int_0^\ell -\left(\frac{m_z}{2} - \frac{\eta M_x}{R}\right)\gamma\, dz \tag{22}$$

The total potential energy functional is

9

$$\pi = U + V = \frac{EI_{Dw}}{2} \int_0^\ell \left(\frac{d^2\gamma}{dz^2} \right)^2 dz + \int_0^\ell \left(\frac{1}{2} k_1 \gamma^2 \right) dz - \int_0^\ell \left(m_z^* - \frac{\eta M_x}{R} \right) \gamma \, dz + \sum_{i=1}^n \frac{1}{2} K_1 \gamma_i^2 \tag{23}$$

Note the discrete nature of the cross-frames in Eq. (23). Applying the Euler-Lagrange differential equation to Eq. (23) yields

$$EI_{Dr} \gamma^{iv} + k_1 \gamma = -\eta \frac{M_x}{R} + m_z^* \tag{24}$$

The relationship between m_z and m_z^* is given by

$$m_z^* = \frac{m_z hc}{2A_0} \tag{25}$$

where A_0 is the enclosed area of the box section.

3.   Transverse bending
Once, γ is determined, the values of the moments at the corners are determined by

$$m_{s1} = -\frac{k_1\gamma}{4} \left(1 + \frac{I_u - I_l}{I_u + I_l + 6\frac{h}{b}\frac{I_u I_l}{I_v}} \right) \tag{26a}$$

$$m_{s2} = \frac{k_1\gamma}{4} \left(1 + \frac{I_l - I_u}{I_u + I_l + 6\frac{h}{b}\frac{I_u I_l}{I_v}} \right) \tag{26b}$$

When the moments of inertia of the upper and lower flanges do not differ more than 50 percent, the transverse bending moments can be computed simply by $k_1\gamma/4$ without incurring more than 0.3 percent error. In the case of a non-composite trapezoidal box-girder, the absolute maximum transverse bending moment occurs at the lower end of the web ($m_{s2} \simeq 2k_1\gamma/4$). The distortional angle as a major parameter for transverse bending is inconsequential in modern box-girders designed following Article 6.7.4.3 (AASHTO [9]). The maximum combined distortional angle is used to determine the cross-frame member force using Eq. (11c).

4.   Analogy
Eq. (24) is the governing differential equation of the distortional behavior of a box-girder. However, it is highly impractical to rely on the solution of Eq. (24) for the distortional analysis as most practical curved composite girders vary their cross sections along the girder length (non-prismatic girders) and non-rigid (yielding) internal cross-frames are installed along the span. And it is also likely that the loading will change along the girder. One of the readily available alternatives is to borrow the concept of the analysis of a beam on elastic foundation, of which solution is provided by the matrix (or finite-element) method. The governing equation for the beam on elastic foundation is

$$EI y^{iv} + ky = p \tag{27}$$

The analogies between the variables in Eqs. (24) and (27) are given in Table 1.

Table 1: Analogy between BEF and distortion (adopted from Yoo et al., 2015)

Variables	BEF	Distortion
Displacement	Vertical deflection (m), y	Distortion angle (rad), γ
Rigidity	EI (N-m^2)	$EI_{Dw} = EWA^*$ (N-m^4)
Moment	$M = EIy''$ (N-m)	$M_{Dw} = EI_{Dw}\gamma''$ (N-m^2)
Load	Distributed load, p (N/m)	Distributed torque, m_z^* (N-m/m)
Distributed resistance	Foundation constant, k (N/m^2)	Frame stiffness, k_1 (N-m/m)
Concentrated resistance	External spring, K (N/m)	Diaphragm stiffness, K_1 (N-m)

5.   Modeling

Although the structural response of torsion and distortion does not occur sequentially in real structures, it is conducive to consider that way for an easier understanding of the phenomenon of distortion of box sections. The developed procedure is equally applicable to straight box-girders by setting the radius of curvature R a very large value. As distortion is induced by the torsional moment, an elastic analysis of the structure on the basis of the assumption that the structure retains its original cross-section shape is a prerequisite for the distortion analysis. It is noted that the static analysis of horizontally curved box-girders can be performed exactly by CVSTB (Yoo, 1979). Once the vertical bending moments are determined from the static analysis, these moments are transformed into equivalent torsional moment as per Eq. (14) and are used as loading terms in the plane-frame analysis (BEF analogy). In the case of straight box-girders, no static analysis is required. A plane-frame analysis program (BEF analogy), however, is not developed using a stiffness matrix based on the solution of the homogeneous governing differential equation (Eq. 24), a reasonable grid refinement appears to be needed. Experience has shown that a minimum of four elements between two adjacent cross-frames is required. The foundation modulus is reflected in the plane-frame program by a series of springs at each node (with the spring constant being simulated by an equivalent truss element) and the stiffness of an internal cross-frame is reflected likewise at the cross-frame location.

Although a minimum of four elements is required between the two adjacent cross-frames, it is preferable to have more elements for accurate evaluation of the distortional warping moment. If the distributed cross-sectional resistance (k_1) is simulated by a series of concentrated truss elements, any increase of the number of elements accompanies the concomitant increase of the number of nodes and members. For a continuous-span bridge, this increases the input data preparation substantially. There seems to be an alternative. Since the load effect diminishes rather quickly in beams on elastic foundation, treat each span as an isolated entity with a proper set of boundary conditions reflecting the continuity. For example, the boundary conditions for the end-span should be roller-clamped. Likewise, the interior-span can be simulated with a clamped-clamped condition.   Sample calculations indicate an error less than 5 percent. If this error is unacceptable, the differences of the distortional warping moments from the end-span, and the interior-span can be readily adjusted at the common interior support by a simple comparison of the output. Since it is highly unlikely that the cross-frame stiffness is so high that there will be practically no distortional angular deformation at the cross-frame location, the maximum

distortional warping moment will always occur at the interior support(s) as will be shown later in the **Major design example**. Hence, this adjustment can be made readily.

6. Major design example

An example design of a horizontally curved box-girder bridge was included in the Guide Specifications (AASHTO, 2003), and the same example has been re-examined in NCHRP Project 12-52 (Kulicki et al., 2005). The same example design is revisited herein to demonstrate the derived procedure. The structure is a three-span-continuous bridge with a radius of curvature 213.4 m long to the center of the bridge. The typical bridge cross-section and the plan are shown in Figs. 6 and 7, respectively. Since the girder is non-prismatic, any analysis aids are not likely to be applicable and a finite-element analysis, other than that having a curved beam element with seven degrees of freedom, is not likely to be able to isolate the warping normal stress component from the stress output. A curved beam element given by Yoo (1979) can be used for this analysis. Section properties are given in Tables 4 and 5. The node and section numbers in these tables are represented in Fig. 7.
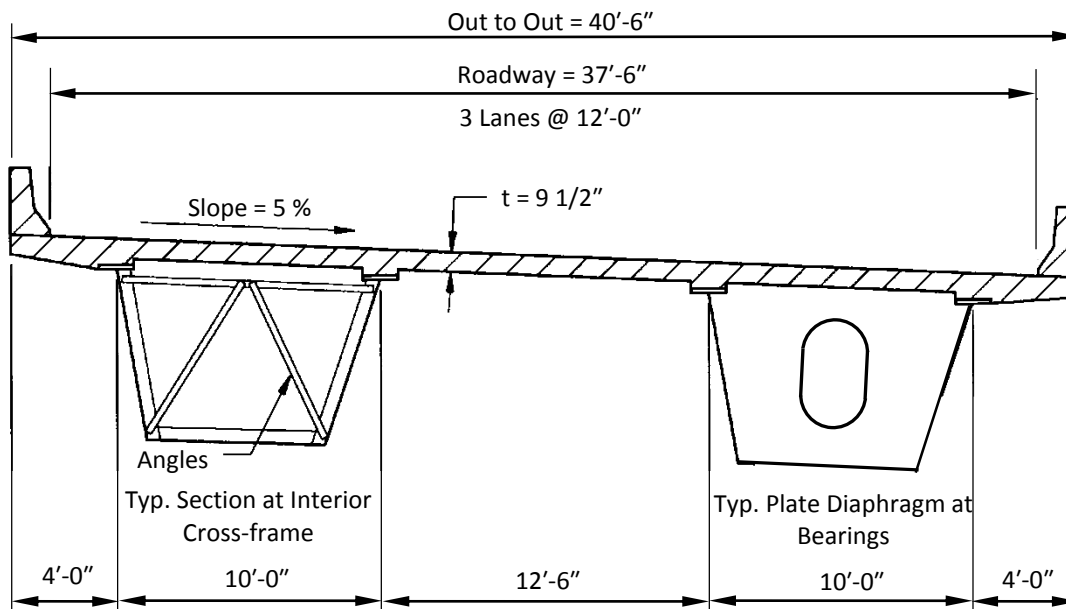
Figure 6: Box-girder bridge cross section (1 in. = 25.4 mm; 1 ft. = 0.3048 m)

6.1   Normal stresses due to warping torsion

Since the procedure to evaluate the normal stresses due to warping torsion is detailed elsewhere (Galambos 1968; Heins, 1975; Nakai and Yoo, 1988), only the end results are presented. Although it is generally perceived that the warping torsion is negligibly small in closed cross-sections, it would be interesting to show just how small the warping normal stress is in the outside girder (the girder farther away from the center of curvature) of the example bridge shown in Fig. 7. The equivalent thickness of the Warren type single diagonal system is given by (Kollbrunner and Basler, 1969)
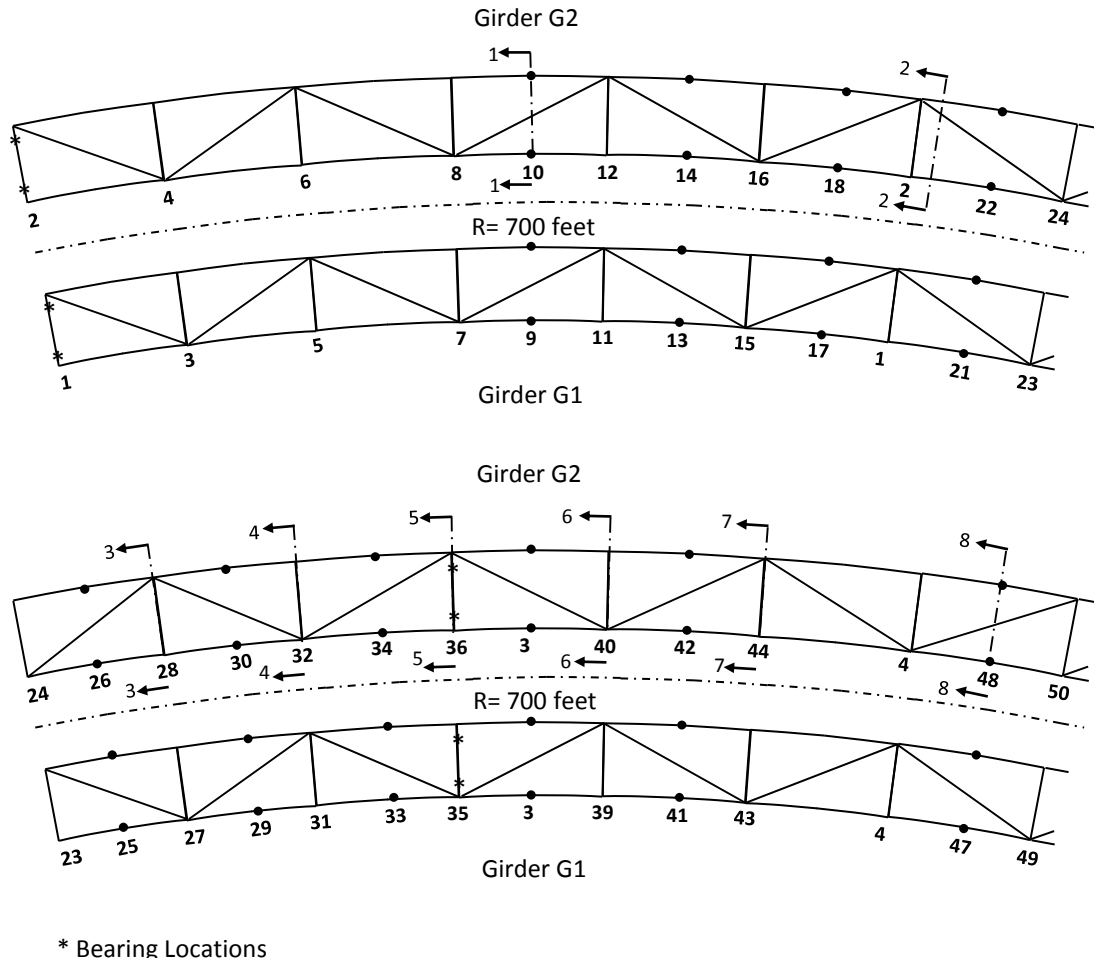
Figure 7: Node and section numbering scheme (1 ft. = 0.3048 m)

$$t^* = \frac{E}{G} \frac{ab}{\dfrac{d^3}{A_d} + \dfrac{2}{3}\dfrac{a^3}{A_f}}$$ (28)

where $E = 200$ GPa, $G = 77$ GPa, $a =$ cross-frame spacing, 4.96 m, $b =$ width of the tub at the top of the web, 3.05 m, and $d =$ that is computed to be 5.83 m. It is noted that the placement of a single diagonal bracing increases the St. Venant torsional constant 3,174 and 227 times that of the unbraced section for Section 1-1 and 5-5, respectively. Values for live load (HL-93) include 33% of dynamic load allowance as per Article 3.6.2 (AASHTO, 2014). A distribution of a live load factor of 1.467 is incorporated for live load moments and bimoments as per Article 4.6.2.2.2 along with a multiple presence factor of 0.85 as per Article 3.6.1.1.2 (AASHTO, 2014). As it appears that the cumulative steel stress at the bottom of the box-girder at the pier is most critical, both bending and warping normal stresses are evaluated at that location. The normal stresses due to bending and torsional warping are tabulated in Table 2. Sample calculations for both stresses are shown below:

13

$$\sigma_b = \sum \frac{\gamma(M)(\bar{y})}{I}$$

$$= -\left\{ \frac{1.25(20,580)(.9858)}{.1827} + \frac{\left[1.25(2,780)+1.5(2,920)\right](1.01)}{.1893} + \frac{1.75(10,699)(1.055)}{.2016} \right\} \quad (29)$$

$$= -278,700\text{kPa} = -279 \text{ MPa} \,(-40.5 \text{ ksi})$$

$$\sigma_w = \sum \frac{\gamma(BM)(W_n)}{I_w}$$

$$= \frac{1.25(146)(-.7160)}{.03929} + \frac{\left[1.25(-135)+1.5(8.64)\right](.0540)}{.02452} + \frac{1.75(32.3)(.599)}{.03885} \quad (30)$$

$$= -3,697 \text{ kPa} \,(+\,0.536\text{ksi}) \text{ or } +900 \text{ kPa} \,(+0.13 \text{ ksi})$$

(compression at the innert corner of the bottom flange)

where σ_b = bending normal stress, σ_w = warping normal stress, γ = load factor, M = bending moment, BM = bimoment, W_n = normalized warping function, and I_w = warping torsion constant.

As can be seen from Table 2, this example bridge meets AASHTO (2014) requirements of C6.7.4.3. Since the exterior girders are continuously braced by the deck and or the lateral bracing and there is no torsional load when the bridge is fully loaded, it would seem reasonable to take only 50 percent of the bimoment computed for the isolated exterior girder. The parapet still creates the highest ratio of the warping to bending stress ratio due to its highly unusual loading of a high torque with a relatively low vertical load. However, the warping stress is less than 1% of the specified yield stress; it may be ignored. The warping stress due to the dead load may be of concern. The curvature effect can best be represented by the subtended angle of each span. The center span of the example bridge adjusted according to Article 4.6.1.2.4b divided by the radius yields a subtended angle of only 13.75 degrees. It has been reported that bridges with subtended angles well over 90 degrees have been built, and the torsional effects are getting progressively severe with increasing subtended angles. For example, the vertical bending moment increased by 1.7% whereas the bimoment increased 241% in the case of dead load analysis in the example bridge by decreasing the radius of curvature 50% (or doubling the subtended angle). With this examination, it can be concluded that the warping normal stress cannot always be ignored but must be checked for bridge girders with large subtended angles, particularly for the non-compact condition under dead load.

Internal cross-frames will not reduce the warping normal stresses. External bracings between boxes are effective. Although external bracings are eschewed in the construction industry, because of the added construction cost and the adverse effect against fatigue, they may offer unique solutions to remedy the high warping stresses. Kim and Yoo (2006c) studied the effectiveness of the external bracings. In addition to the debate, whether a single box-girder ramp is a facture-critical structure or not, the inability to install external bracings may limit the subtended angles of the spans in the ramp structure.

Table 2: Moments and bimoments at interior support (adopted from Yoo et al., 2015)

Loading Case	Moment	Bimoment	σ_b	σ_w	$\sigma_w / \sigma_b \; (\%)$
Dead Load	-20,580	+146.0	-138.8	-3.33	2.40
Parapet	- 2,780	-135.0	-18.5	-0.37	2.00
FWS	-2,970	+8.64	-23.4	+0.03	-0.13
Live load	-10,699	+32.3	-98.0	+0.87	-0.89
Total			-278.7	-3.70/+0.90	+4.40/-1.02

Notes: Moments are in kN·m; bimoments are in kN·m^2; and stresses are in MPa.
    Moment and bimoments are unfactored. Stresses are multiplied by the proper load factors.
    It is noted that normal stresses due to bimoments are computed based on uncracked section properties.

Legend: FWS =future wearing surface

6.2   Distortional stresses
Article 6.7.4.3 (AASHTO [9]) mandates that the sum of torsional warping stress and distortional warping stress must be less than 10 percent of the vertical bending stress at the strength limit state. The provision also stipulates that the transverse bending stress due to distortion be less than 138 MPa (20 ksi). The Hanshin Guidelines (Hanshin, 1988) require that the sum of the warping and distortional normal stresses to be less than five percent of the bending stress. Other than relying on very complex and expensive refined analysis methods, there has not been an easy-to-apply methodology to check the distortional stresses of horizontally curved box-girders.

Bethlehem Designer's guide (Heins and Hall, 1981) is perhaps the only design aid for the distortional analysis. However, the guide is based on the BEF analogy, which is originally developed by Wight et al. (1968) for straight box-girders. As it will be discussed later, applying the BEF analogy developed for straight box-girders to horizontally curved box-girders is grossly unconservative. Although Dabrowski (1972) extended the concept to horizontally curved box-girders (with a sign error in a loading term), he relies heavily on the copious design tables and charts to solve the resulting fourth order differential equation with constant coefficients analogous to the governing differential equation for beams on elastic foundations. One rarely sees modern horizontally curved prismatic box-girder bridges aligned on a simple span or two equal spans. These are the type of structures included in Dabrowski's design aids.

As demonstrated by Kim and Yoo (2006a, 2006b, 2009), the cross-frame spacing cannot be determined by distortional stress level alone in the case of horizontally curved tub girders. The spacing has a major implication to the design of top lateral bracing members, which may require a heavy section if an unfavorable deck casting sequence is considered. Furthermore, the diaphragm or the cross-frame stiffness has a major implication on the cross-frame spacing. In fact, the cross-

frame stiffness used in the example design is only 4 percent of the solid diaphragm that is considered to be close to the rigid one.

The procedure developed herein does not have afore-mentioned limitations or drawbacks. It is straight forward and simple enough requiring only two ordinary computer programs, which should be readily available in the literature. An application of the developed procedure is demonstrated here using an example bridge.

K-truss internal cross-frames are used in the example bridge. The K-frames are spaced longitudinally at approximately 4.88 m (measured along the centerline of the bridge). The maximum member force was found to be 785 N (80 kips) in the diagonal (AASHTO, 2003) under the factored loads. In this analysis, a single angle, L178x100x13 (L7x4x1/2) having an area of 3.28125E-03 m^2 (5.25 in^2) is used for the diagonals of the K-frames. The diagonals are locked in the initial stress as outlined in recent publications (Kim and Yoo, 2006a; 2006b; 2009) under the dead load, and additional stresses are added following the distortional action under dead load, superimposed dead load, and vehicular live load.

As per Article 6.7.4.3 (AASHTO, 2014), it is assumed that there are full-depth internal and external diaphragms provided at support lines. Therefore, no distortion is allowed there in the model. A typical K-frame stiffness is computed according to Eq. (11c) as

$$\ell_b = 0.0254\sqrt{78^2 + (81/2)^2} = 2.23 \text{ m } (87.9 \text{ in.})$$

$$K_1 = \frac{EA_b c^2 h^2}{2\ell_b^3} = \frac{200x10^9 \left(5.25x0.0254^2\right)\left(81x0.0254\right)^2 \left(78x0.0254\right)^2}{2(2.23)^3} = 5.075 \times 10^8 \text{ N} \cdot \text{m} \qquad (31)$$

The cross-sectional stiffness for each different section (with a unit of $N \cdot m/m$) as the equivalent foundation moduli is computed according to Eq. (13) and tabulated in Table 3. As can be seen from Table 3, k_1 is in the order of 1/1,000 of K_1. Examination of a series of analysis results reveals that the primary controlling parameter for the distortional warping moment and transverse bending is K_1. Doubling or tripling k_1 hardly affects the results, thereby justifying the assumption employed by Wright et al. (1968).

It is convenient to assume the member length (ℓ) of the fictitious truss simulating the elastic foundation to be 1 m. Hence, the equivalent axial stiffness or the spring constant is

$$K_1 = \frac{A_{K_1} E}{\ell} = A_{K_1} E \qquad (32)$$

$$A_{K_1} = K_1 / E = 5.075 \times 10^8 / 200 \times 10^9 = 2.5375 \times 10^{-3} \text{ m}^3 \qquad (33)$$

$$A_{k_1} = \ell_b k_1 / E \qquad (34)$$

where ℓ_b is the length of the beam element.

It is recalled that the right side of Eq. (24) is $-\eta M_x / R + m_z *$ having a unit of $N \cdot m/m = N$. As most plane-frame programs are designed to provide work-equivalent nodal forces at each node, the distributed torsional moments of the right side are transformed into concentrated nodal torques having a unit of $N \cdot m$ by multiplying the value by the length of the element (beam). This operation

can be tedious and time-consuming. Software such as Excel and TextPad can expedite this operation greatly.

Table 4 summaries the six loading cases considered for the example bridge; three dead load and three live load cases. These are the steel and deck concrete dead load, future wearing surface, and parapet and three truck positions for the maximum moment in the end span, at the pier, and the center of the interior span. Fig. 8 shows the variation of the distortional warping moments for these six loading cases. Since the maximum distortional warping moments occur at the first interior pier, all of the variations are plotted in the first end span except for the loading case for the maximum negative moment at the pier, for which the variations of the distortional warping moments are shown for the interior span. Sample calculation for the distortional warping stress is shown below:

$$
\begin{aligned}
\sigma_{Dw\,\text{DL}} &= \sum \frac{\gamma\left(M_{Dw}\right)\left(w_D\right)}{I_{Dw}} \\
&= \frac{1.25\left(-7.99E+04\right)\left(-0.949\right)}{0.0391} = +2.42\ \text{MPa}
\end{aligned}
\tag{35}
$$

where distortional section properties are given in Table 3.

As shown in Table 4, the sum of the negative distortional warping normal stresses is slightly greater than that of the positive value; the sum of the negative stresses will have a cumulative effect on the bottom of the inner web to the vertical bending stresses. Here again, it is recalled that the importance of tracking the proper sign in Eq. (14) to distinguish whether the stresses are to be additive or subtractive to the vertical bending stresses.

As shown comparatively in Tables 2 and 4, it becomes clear that the torsional warping stresses are slightly greater than the distortional warping stresses in this example bridge, and appears to be the case for most properly braced horizontally curved bridges. It is recalled that when the box section is square, there is no torsional warping stresses developed, and the sentiment of Eurocode (2006) provision to permit ignoring the warping torsion entirely is understandable. However, this provision is somewhat unconservative as the subtended angle of a curved span gets large; the normal stress due to the torsional warping moment (bimoment) becomes non-negligible.

The sum of normal stresses due to torsional warping and distortional warping, 7.10 MPa, is only 2.55 percent of the total vertical bending stress. Hence, the design meets the requirement (less than 10 percent of the vertical bending stress) of Article 6.7.4.3 (AASHTO, 2014). It appears that the area of the cross-frame used in this example can easily be reduced by 50%. It is noted that both the cross-frame stiffness and spacing play an important role in controlling box distortion.

6.3 Transverse bending stresses
The transverse bending stress due to distortional warping is a function of the distortional angle. The maximum angle occurs somewhere between the two end supports of each span. If the cross-frame stiffness is not too stiff, it usually develops near the center of the span. For the strength limit state (Strength I), the maximum transverse bending stress develops near Section 1-1 (see Fig.

Table 3: Distortional section properties (adopted from Yoo et al., 2015)

Section Node	Section Size	Section Type	β	w_{D1} (m^2)	I_{Dw} (m^6)	k_1 (Nm/m)	α_0	α_1	α_2	η
1-1 10	2-406x25.4 2-2042x14 2108x16 A=111529 t^*=1.11	Noncomp	1.576	0.541	0.0201	103848	5.8624	0.0826	0.2770	0.0353
		Comp DL	2.642	0.367	0.0292	183256	2.9634	0.2533	0.0322	0.2413
		Comp LL	4.850	0.220	0.0360	365373	1.4863	0.3157	0.0365	0.2911
3-3 28	2-457x38.1 2-2042x14 2108x25.4 LS WT203x43.5 A=150962 t^*=1.23	Noncomp	1.788	0.494	0.0268	152772	3.9850	0.0398	0.1424	0.0040
		Comp DL	2.712	0.359	0.0358	252537	2.1611	0.2157	0.0118	0.2103
		Comp LL	4.634	0.229	0.0435	459461	1.1844	0.2664	0.0053	0.2619
5-5 36	2-457x76.2 2-2042x14 2108x38.1 LS WT203x43.5 A=212557 t^*=1.32	Noncomp	2.384	0.398	0.0391	226226	2.6912	-0.0776	0.0404	-0.0926
		Comp DL	3.169	0.317	0.0465	242999	2.2144	0.0385	0.0100	0.0339
		Comp LL	4.805	0.222	0.0541	488105	1.1024	0.2136	0.0005	0.2132
8-8 48	2-406x25.4 2-2042x14 2108x19 A=118193 t^*=1.11	Noncomp	1.504	0.558	0.0213	122196	4.9821	0.1371	0.2620	0.0846
		Comp DL	2.522	0.381	0.0309	204819	2.6604	0.2849	0.0247	0.2756
		Comp LL	4.630	0.229	0.0383	408846	1.3328	0.3855	0.0196	0.3708

Notes: Areas are in mm^2; length, width, and thickness are in mm. Cracked sections are not considered separately as they are effective for torsion.

Legend: β =location of the distortional center; w_{D1}= distortional warping function at the inner top flange defined in Fig. 4;

I_{Dw} = distortional warping constant in m^6; k_1= stiffness of the cross section against distortion; α_0= coefficient;

α_1 = coefficient; α_2= coefficient; and η = conversion coefficient

Noncomp = steel section only

Comp DL = steel section plus concrete deck transformed using modular ratio of 3n

Comp LL = steel section plus concrete deck transformed using modular ratio of 1n

7). The maximum factored transverse bending stress is 0.6 MPa, which is negligibly small compared with the maximum permissible value of 138 MPa (20 ksi).

It is of interest to note that Kulicki et al. (2005) report that the maximum transverse bending stress range of 3.45 MPa (0.5 ksi) for the fatigue check near the interior support. In light of the fact that the distortional angle is usually very small near the support because of the presence of a solid diaphragm, the reported location of the maximum transverse bending stress range is quite unusual. In this study, the maximum fatigue stress range is found to be 0.6 MPa (0.1 ksi) near the center of the interior span.

6.4 Stiffness of the cross-frame
Examination of the plan (Fig. 7) reveals that there is no possibility of increasing the cross-frame spacing from what it is now. Any increase of the cross-frame spacing necessitates the top diagonal to make an angle less than 30 degrees with the top flange; thereby making it quite inefficient in resisting the panel shear (the tendency to bulge the top flanges out). Reducing the current spacing does not appear to be a viable option either as it puts an undue additional fabrication expense. There seems to be an alternative means to adjust the cross-frame spacing by adjusting the cross-frame stiffness. When the area of the cross-frame member was doubled (increased 100 %) in the dead load analysis in this example bridge, the maximum distortional warping moment decreased by 17.7 percent.

7. Concluding remarks
A procedure based on an analogy with the theory of beams on elastic foundation is developed for the analysis of distortion induced stresses of horizontally curved box-girders. Many new equations have been developed for trapezoidal tub-girders with overhangs as pertinent equations are not

Table 4: Distortional warping moments ($N \cdot m^2$) and stresses (MPa) (adopted from Yoo et al., 2015)

Loading Cases	M_{Dw}	w_{D2} (m^2)	I_{Dw} (m^6)	σ_{Dw} (MPa)	L Factor
Dead Load	-7.99E+04	-0.9488	0.0391	+2.42	1.25
FWS	+7.00E+03	-1.0046	0.0465	-0.23	1.50
Parapet	-2.42E+04	-1.0046	0.0465	+0.65	1.25
LL, $+M_{es}$	+4.95E+04	-1.0667	0.0541	-1.71	1.75
LL, $-M$	+1.56E+04	-1.0667	0.0541	-0.54	1.75
LL, $+M_{cs}$	+2.67E+04	-1.0667	0.0541	-0.92	1.75
Sum				+3.07/-3.40	

Notes: $w_{D2} = -\beta \left(w_{D1} \right)$

Legend: M_{Dw} = distortional warping moment; σ_{Dw} = distortional warping normal stress;

M_{es} = truck position for the maximum positive moment in the end span;

M_{cs} = truck position for the maximum positive moment in the center span;

L Factor = load factor
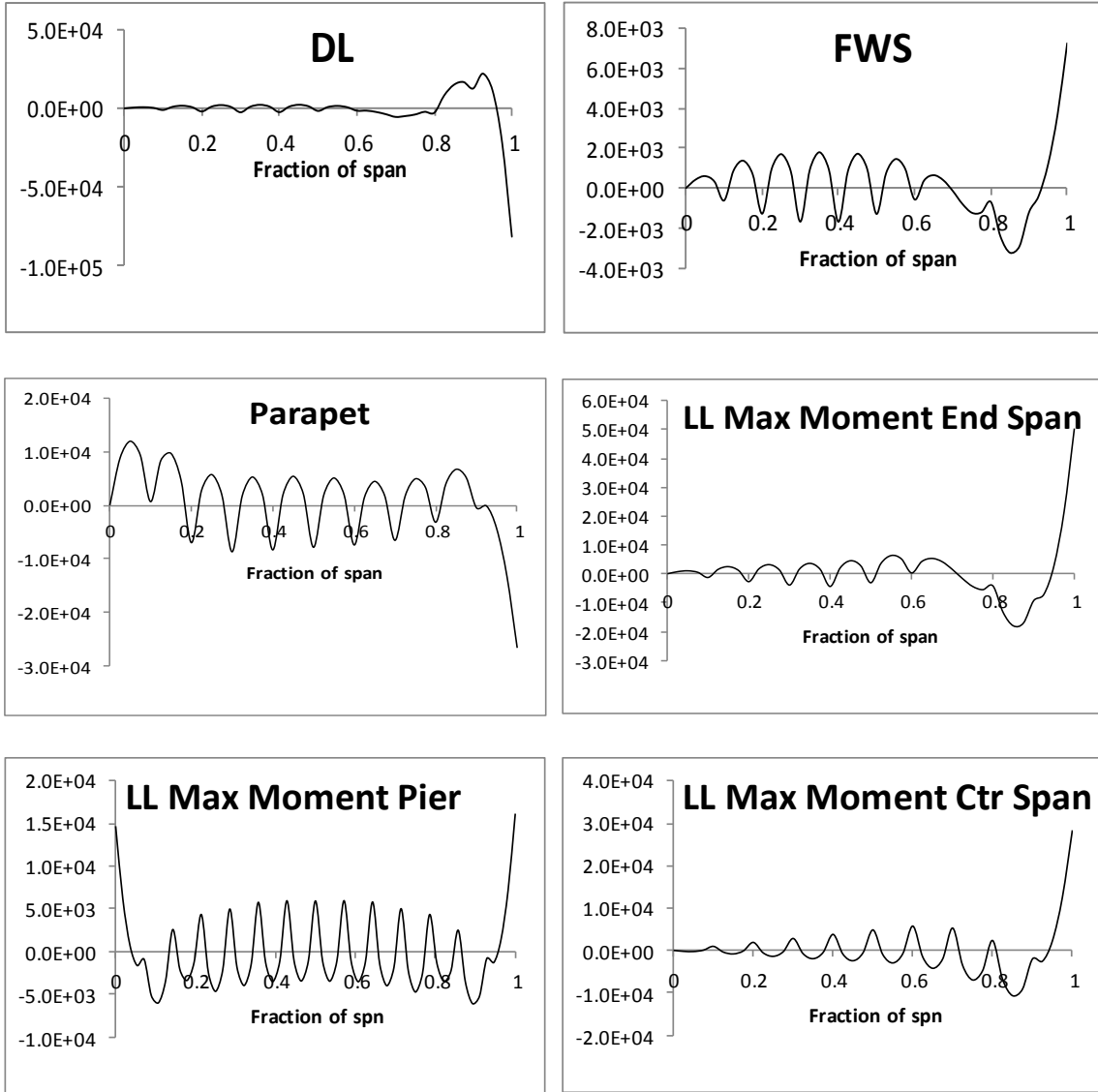
Figure: 8 Variations of distortional warping moments ($\text{N} \cdot \text{m}^2$) (adopted from Yoo et al., 2015)

available elsewhere. The procedure is capable of handling simple or continuous single cell box-girders (or separated multi-cell box-girders) with rigid or deformable interior diaphragms or cross-frames.

Examples show that distortional stresses can be quite significant in horizontally curved steel box-girders, particularly, in spans with large subtended angles. Although the maximum cross-frame spacing is increased from 9 m (30 feet, AASHTO, 2003) to 12 m (40 feet, AASHTO, 2014), Article 6.7.4.3 (AASHTO,2014) stipulates to check torsional, distortional warping stresses and transverse bending stresses induced by distortion and the procedure developed herein meets this requirement.

Refined analytical methods, for example, a three-dimensional nonlinear incremental finite-element method, are available for evaluation of these stresses. However, the enormous efforts required in

the preparation of the modeling and computation tends to conceal the design parameters. In the plane-frame (BEF analogy), the analysis results become readily available and different cross-frame spacing can be tried with a minimal effort by replacing the cross-frame stiffness with the property of the spring used to represent the foundation modulus.

Maximum bending moments develop when the bridge is fully loaded in all lanes with dead and live load plus impact. Warping stresses induced by the small torsional component may be accounted for by a few percent of the flexural stress. When a bridge is loaded by a single vehicle, it may create a high torsional component and may affect adversely the fatigue behavior. The procedure developed herein can effectively be utilized to analyze this situation.

Acknowledgements

References

Abbas, H., Sause, R., and Driver, R.G. (2006). "Behavior of corrugated webb I-girders under in-plane loads," *Journal of Engineering Mechanics*, ASCE, 132(8): 806-14.

American Association of State Highway and Transportation Officials (1980). "Guide Specifications for Horizontally Curved Highway Bridges, "American Association of State Highway Officials, Inc., Washington, D.C.

American Association of State Highway and Transportation Officials (2002). "Standard specifications for highway bridges," 17th ed., Washington, DC.

American Association of State Highway and Transportation Officials (2003). "AASHTO Guide specifications for horizontally curved steel girder highway bridges with design examples for I-girder and box-girder bridges," Washington, DC.

American Association of State Highway and Transportation Officials (2014). "AASHTO LRFD bridge design specifications," 7th ed., Washington, DC.

Dabrowski, R. (1968). "Gekrümmte dünnwandige Träger," Springer-Verlag, Belin /Heidelberg /New York.

Dabrowski, R. (1972). "Curved thin-walled girders," translated version from the German Edition (Springer-Verlag, 1968) by Amerongen, Cement and Concrete Association, London.

Eurocode 3 (2006). "Design of steel structures – Part 1-5: Plated structural elements," European Committee for Standardization, Brussels, Belgium.

Fan, Z., and Helwig, T.A. (1999). "Behavior of steel box girders with top flange bracing," Journal of Structural Engineering, ASCE, 125(8), 710-18.

Fan, Z., and Helwig, T.A. (2002). "Distortional loads and brace forces in steel box girders," Journal of Structural Engineering, ASCE, 128(6), 829-37.

Galambos, T.V. (1968).Structural members and frames, Englewood Cliffs, NJ: Prentice-Hall.

Hanshin Expressway Public Corporation. (1988). "Guidelines for the design of horizontally curved girder bridges (draft)," Hanshin Expressway Public Corporation and Steel Struct Study Com, Osaka, Japan (in Japanese).

Heins, C.P, and Hall, D.H. (1981). Designer's guide to steel box-girder bridges, Bethlehem Steel Corporation, Bethlehem, PA.

Heins, C.P. (1975). Bending and torsional design in structural members, Lexington Book, Lexington, MA.

Kermani, B., and Waldron, P. (1993). "Analysis of continuous box girder bridges including the effects of distortion," *Computers and Structures*, 47(3): 427-460.

Kim, K., and Yoo, C.H. (2006a). "Brace forces in steel box girders with single diagonal lateral bracing systems," *Journal of Structural Engineering*, ASCE, 132(8): 1212-22.

Kim, K., and Yoo, C.H. (2006b). "Interaction of top lateral and internal bracing systems in tub girders," *Journal of Structural Engineering*, ASCE, 132(10): 1611-20.

Kim, K., and Yoo, C.H. (2006c). Effects of external bracing on horizontally curved box girder bridges during construction, Engineering Structures; 28(12): 1650-7.

Kim, K., and Yoo, C.H. (2009). "Bending behavior of quasi-closed trapezoidal box-girders with X-type internal cross-frames," *Journal of Constructional Steel Research*, 65: 1827-35.

Kollbrunner, C.G, and Basler K. (1969). Torsion in structures, an engineering approach, translated from German edition by E.C. Glauser with annotation and an appendix by B.G. Johnston, Spriger-Verlag.

Kulicki, J.M., Wassef, W.G, Smith, C, and Johns, K. (2005). AASHTO-LTFD Design Example, Horizontally Curved Steel Box-girder Bridge, Final Report, NCHRP Project 12-52, NCHRP, TRB, Modjeski and Masters, Inc., Harrisburg, PA.

Nakai, H, and Yoo, C.H. (1988). Analysis and design of curved steel bridges, New York, NY: McGraw-Hill Book Company.

Nakai, H, and Murayama, Y. (1981). "Distortional stress analysis and design aid for horizontally curved box girder bridges with diaphragms," *Proceedings of the Japanese Society of Civil Engineers*, (309): 25-39 (in Japanese).

Park, N., Choi, S., and Kang, Y. (2005a). "Exact distortional behavior and practical distortional analysis of multicell box girders using an expanded method," *Computers and Structures*, 83(19-20): 1607-1626.

Park, N., Choi, Y., and Kang, Y. (2005b). "Spacing of intermediate diaphragms in horizontally curved steel box girder bridges," *Finite Elements in Analysis and Design*; 41(9-10) : 925-943.

Park, N., Lim, N., and Kang, Y. (2003). "A consideration on intermediate diaphragm spacing in steel box girder bridges with a doubly symmetric section," *Engineering Structures*, 25(13): 1665-1674.

Timoshenko, S. (1955). Strength of materials, Part I, Elementary Theory and Problems, 3rd ed., Princeton, NJ: D. Van Nostrand Company.

Wright, R.N., Abdel-Samad, S.R., and Robinson, A.R. (1968). "BEF analogy for analysis of box-girders," *Journal of Structural Div. ASCE*, 94(7): 1719-43.

Yoo, C.H. (1979). "Matrix formulation of curved girders," *Journal of Engineering Mechanics Div. ASCE*, 105(6): 971-88.

Yoo, C.H., Kang, J., and Kim, K., (2015). "Stresses due to distortion on horizontally curved tub-girders," *Engineering Structures* (to be published).